

BCS theory for s+g-wave superconductivity in borocarbides Y(Lu)Ni₂B₂CQingshan Yuan^{1,2} and Peter Thalmeier¹¹ Max-Planck-Institut für Chemische Physik fester Stoffe, Nöthnitzer Str. 40, 01187 Dresden, Germany² Pohl Institute of Solid State Physics, Tongji University, Shanghai 200092, P.R.China

The s+g mixed gap function $\Delta_{\mathbf{k}} = \Delta[(1-x) - x \sin^4 \theta \cos 4\phi]$ (x : weight of g-wave component) has been studied within BCS theory. By suitable consideration of the pairing interaction, we have confirmed that the coexistence of s- and g-wave, as well as the state with equal s and g amplitudes (i.e., $x = 1/2$) may be stable. This provides the semi-phenomenological theory for the s+g-wave superconductivity with point nodes which has been observed experimentally in borocarbides YNi₂B₂C and possibly in LuNi₂B₂C.

PACS numbers: 74.20.Rp, 74.20.Fg, 74.70.Dd

I. INTRODUCTION

The rare earth nickel borocarbides RNi₂B₂C (R=Y, Lu, Tm, Er, Ho, and Dy) have attracted great interest in recent years due to superconductivity (SC) as well as its possible coexistence with antiferromagnetic order.^{1,2} It has initially been thought that these materials can be understood by an isotropic s-wave pairing via the conventional electron-phonon coupling.³ However, recent various experimental results particularly on the two non-magnetic borocarbides Y(Lu)Ni₂B₂C, including specific heat,⁴⁻⁷ thermal conductivity,^{8,9} Raman scattering,¹⁰ NMR relaxation rate,¹¹ photoemission spectroscopy,¹² scanning tunneling microscopy and spectroscopy,¹³ have unambiguously shown that the gap function is highly anisotropic with anisotropy ratio⁸ $\Delta_{min}/\Delta_{max} \leq 10^{-2}$. For example, the \sqrt{H} dependence of the specific heat in the vortex state indicates a superconducting state with nodal excitations⁴⁻⁶. The T^3 power law behavior of the spin-lattice relaxation rate¹¹ also suggests the existence of nodes. Very recently, compelling evidence is presented by Izawa *et al.* from the angular-dependent thermal conductivity in a magnetic field that the gap function of YNi₂B₂C has point nodes which are located along the [1,0,0] and [0,1,0] directions.⁸ The same conclusion can be also drawn from the angular-dependent specific heat data.⁷ Highly anisotropic s-wave gap (with possible nodes) was also discovered in LuNi₂B₂C by thermal conductivity measurements as a function of temperature and field strength.⁹ Thus the previous isotropic s-wave theory has to be critically reconsidered.

Recently Maki *et al.* have proposed that the so called s+g-wave spin singlet gap function for Y(Lu)Ni₂B₂C superconductors, i.e.,^{14,15,8}

$$\Delta_{\mathbf{k}} = \frac{\Delta}{2}(1 - \sin^4 \theta \cos 4\phi), \quad (1)$$

is consistent with experimental results. We introduced θ, ϕ as polar and azimuthal angles of \mathbf{k} , respectively. Here the second 'g-wave' contribution is given by a fourth degree fully symmetric (A_{1g}) basis function $\psi^{(4)}(\theta, \phi)$ in tetragonal D_{4h} symmetry which is, up to a constant, equal to the real 'tesseral harmonic' $Z_{44}^c(\theta, \phi) = (1/\sqrt{2})[Y_4^4(\theta, \phi) + Y_4^{-4}(\theta, \phi)]$ function. We have

$$\psi^{(4)}(\theta, \phi) = k_x^4 + k_y^4 - 6k_x^2 k_y^2 = \sin^4 \theta \cos 4\phi. \quad (2)$$

In the gap function (1), the amplitudes of s- and g-components are assumed to be equal. Thus 4 (and only 4) point nodes at $\theta = \pi/2$ and $\phi = 0, \pi/2, \pi, 3\pi/2$ are realized, see the middle panel of Fig. I. This is exactly what has been observed experimentally.⁸

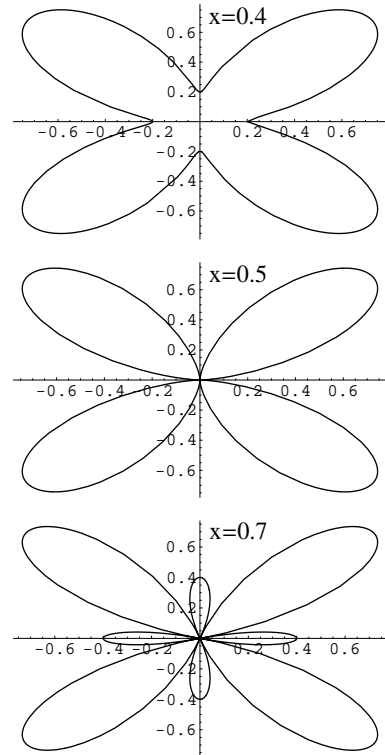


FIG. 1. The xy -plane ($\theta = \pi/2$) polar plots of the s+g wave gap $|\Delta_{\mathbf{k}}|$ for various tuning parameter x .

On the other hand, there is no symmetry reason for the constraint of equal amplitudes of s and g. More generally, the s+g gap function is:

$$\Delta_{\mathbf{k}} = \Delta[(1-x) - x \sin^4 \theta \cos 4\phi] = \Delta f(\theta, \phi) \quad (3)$$

with a tuning parameter x characterizing the weight of g-wave component. Obviously Eq. (1) corresponds to the

special case $x = 1/2$. If $x < 1/2$, s-wave is dominant and the nodes will be removed; while if $x > 1/2$, g-wave has strong weight and will contribute 8 line nodes. The three different cases have been shown in xy -plane in Fig. 1.

A natural question then arises how to understand the origin of the above s+g hybrid pairing. So far, a microscopic theory for the pairing potential is not available which might be complicated due to the complex Fermi surface of borocarbides¹⁶ and the possibility of strongly anisotropic Coulomb interactions. As a first step, however, it is necessary to investigate phenomenologically how the s+g state can be realized by constructing an appropriate pairing potential. This is the topic of the present work. Within BCS weak-coupling theory we will show how a stable coexistence of s- and g-wave and in particular how the fine tuning $x = 1/2$ (s+g) can be realized almost independent of temperature below T_c .

A similar issue has been addressed by Lee and Choi¹⁷ in their theory to explain Raman scattering data, but no complete analysis was presented. First, they do not consider the θ -dependence of the g-wave part, i.e., implicitly assume a gap function with cylindrical symmetry. Second, they use gap models with strong g-component. As shown before in Fig. 1, these will exhibit 8 line nodes, which are inconsistent with the experimental results⁸ which have revealed 4 point nodes.

II. PAIRING INTERACTION AND BCS THEORY FOR THE S+G WAVE STATE

In view of the orthogonality of s- and g-wave functions in Eq. (3), one may naturally express the pairing potential as sum of two separable parts whose weight is given by two parameters V_s and V_g :¹⁸

$$V_{\mathbf{k}\mathbf{k}'} = -[V_s + V_g \psi^{(4)}(\theta, \phi) \psi^{(4)}(\theta', \phi')]. \quad (4)$$

Here the unprimed and primed angles correspond to \mathbf{k} and \mathbf{k}' respectively. Each term in Eq. (4) is separable with respect to wavevectors \mathbf{k} and \mathbf{k}' .

Here we try to propose a pairing potential, similar to that used in Ref. 17 for the cylindrical gap, by adding another mixing term V_{sg} :

$$V_{\mathbf{k}\mathbf{k}'} = -[V_s + V_g \psi^{(4)}(\theta, \phi) \psi^{(4)}(\theta', \phi') + V_{sg}(\psi^{(4)}(\theta, \phi) + \psi^{(4)}(\theta', \phi'))]. \quad (5)$$

The reason for the choice of this type of interaction as well as its derivation will be discussed later. We simply adopt it as the model pairing potential for the moment.

The standard BCS gap equation is then written as

$$\Delta_{\mathbf{k}} = - \sum_{\mathbf{k}'} V_{\mathbf{k}\mathbf{k}'} \frac{\Delta_{\mathbf{k}'}}{2E_{\mathbf{k}'}} \tanh(\beta E_{\mathbf{k}'}/2), \quad (6)$$

where $\beta = 1/(k_B T)$ and $E_{\mathbf{k}} = \sqrt{(\varepsilon_{\mathbf{k}} - \mu)^2 + \Delta_{\mathbf{k}}^2}$ is the quasiparticle spectrum. $\varepsilon_{\mathbf{k}}$ is the free electron dispersion,

and μ is the chemical potential. It is easy to check that the gap function (3) is a self-consistent solution of Eq. (6) with inclusion of the pairing interaction (5), if the gap amplitude Δ and tuning parameter x satisfy the following self-consistent equations:

$$1 - x = V_s \sum_{\mathbf{k}} \frac{f(\theta_{\mathbf{k}}, \phi_{\mathbf{k}})}{2E_{\mathbf{k}}} \tanh(\beta E_{\mathbf{k}}/2) + V_{sg} \sum_{\mathbf{k}} \psi^{(4)}(\theta_{\mathbf{k}}, \phi_{\mathbf{k}}) \frac{f(\theta_{\mathbf{k}}, \phi_{\mathbf{k}})}{2E_{\mathbf{k}}} \tanh(\beta E_{\mathbf{k}}/2), \quad (7)$$

$$-x = V_g \sum_{\mathbf{k}} \psi^{(4)}(\theta_{\mathbf{k}}, \phi_{\mathbf{k}}) \frac{f(\theta_{\mathbf{k}}, \phi_{\mathbf{k}})}{2E_{\mathbf{k}}} \tanh(\beta E_{\mathbf{k}}/2) + V_{sg} \sum_{\mathbf{k}} \frac{f(\theta_{\mathbf{k}}, \phi_{\mathbf{k}})}{2E_{\mathbf{k}}} \tanh(\beta E_{\mathbf{k}}/2). \quad (8)$$

where the angles have been indexed by their corresponding wavevector for clarity. Replacing the summation by integration according to

$$\sum_{\mathbf{k}} \simeq \frac{N(0)}{4\pi} \int_{-\hbar\omega_D}^{\hbar\omega_D} d\varepsilon \int d\Omega,$$

where $\hbar\omega_D$ is an energy cut-off to enforce the constraint $|\varepsilon_{\mathbf{k}} - \mu| \leq \hbar\omega_D$ (ω_D : Debye frequency for phonon-mediated SC), and $N(0)$ is the density of states at zero energy for the spectrum $\varepsilon_{\mathbf{k}} - \mu$, we may obtain the following equations:

$$1 - x = \frac{1}{4\pi} (\tilde{V}_s I_1 + \tilde{V}_{sg} I_2), \quad (9)$$

$$-x = \frac{1}{4\pi} (\tilde{V}_g I_2 + \tilde{V}_{sg} I_1). \quad (10)$$

Above, $\tilde{V}_s = N(0)V_s$, $\tilde{V}_g = N(0)V_g$, $\tilde{V}_{sg} = N(0)V_{sg}$ are redefined dimensionless interaction constants, and the integrals $I_{1,2}$ are written as follows

$$I_1 = \int_0^1 d\varepsilon \int d\Omega \frac{f \tanh(\beta \sqrt{\varepsilon^2 + \Delta^2} f^2 / 2)}{\sqrt{\varepsilon^2 + \Delta^2} f^2}, \quad (11)$$

$$I_2 = \int_0^1 d\varepsilon \int d\Omega \psi^{(4)} \frac{f \tanh(\beta \sqrt{\varepsilon^2 + \Delta^2} f^2 / 2)}{\sqrt{\varepsilon^2 + \Delta^2} f^2}, \quad (12)$$

where we use the abbreviated symbols f and $\psi^{(4)}$, and $\hbar\omega_D$ has been taken as the energy unit.

III. NUMERICAL RESULTS

We first consider $V_{sg} = 0$, i.e., we assume the pairing interaction (4). It was found that one or two s+g solutions (i.e., $\Delta > 0$, $0 < x < 1$) may appear when \tilde{V}_g is a few times greater than \tilde{V}_s . On the other hand, it is easy to check that the pure s-wave ($x = 0$) and pure g-wave ($x = 1$) are always trivial solutions. Thus one needs to

compare their free energies to find the stable solution. In unit of $N(0)(\hbar\omega_D)^2$ the free energy is given by

$$F = \frac{-1}{2\pi} \int_0^1 d\varepsilon \int d\Omega [\sqrt{\varepsilon^2 + \Delta^2 f^2} + \frac{2}{\beta} \ln(1 + e^{-\beta\sqrt{\varepsilon^2 + \Delta^2 f^2}})] + \Delta^2(1-x)^2/\tilde{V}_s + \Delta^2 x^2/\tilde{V}_g.$$

Detailed calculation shows that the s+g mixed state is unstable in most of the parameter space. As an example, we have shown in Fig. 2 all the solutions and their relative energies as functions of \tilde{V}_g for fixed $\tilde{V}_s = 0.2$ and $T = 0$. Two s+g solutions may be present, as shown by the dotted and dashed lines. But compared to the pure s- and/or g-wave solutions, they are found to be energetically unfavorable, see the lowest panel in Fig. 2.¹⁹ Thus the s+g mixture seems very unlikely under the pairing interaction which is the sum of two separable parts (4).

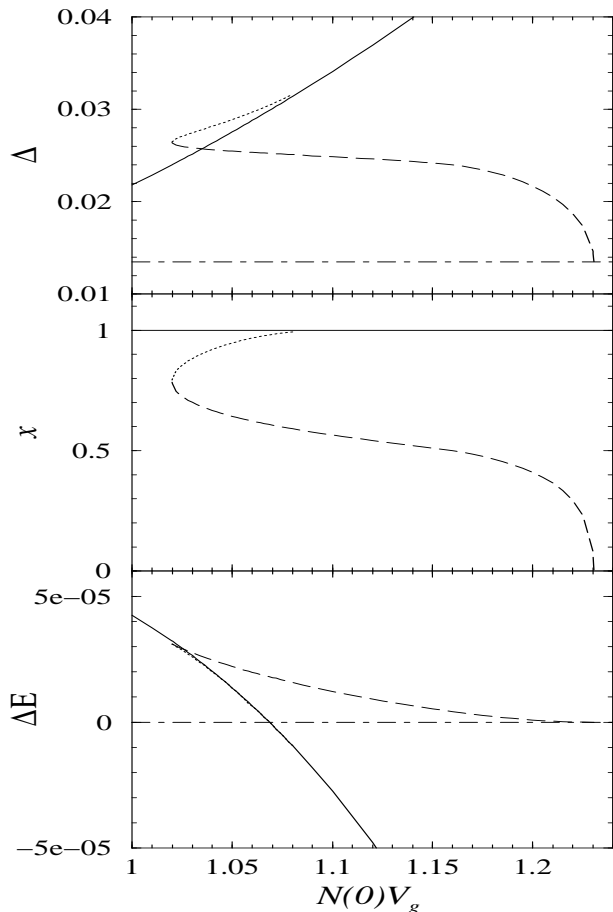


FIG. 2. The values Δ , x , and relative energies ΔE as functions of \tilde{V}_g for $\tilde{V}_s = 0.2$ and $T = 0$. The solid and dot-dashed lines are for pure g- and s-wave solutions, respectively. The dotted and dashed lines are for two possible s+g mixed solutions. The energy of the pure s-wave solution is taken as the reference point in the lowest panel. Energy unit for Δ is $\hbar\omega_D$ and for ΔE is $N(0)(\hbar\omega_D)^2$.

Once $V_{sg} > 0$, the above situation changes substantially. In this case the pure s- and g-wave are no longer

solutions of Eqs. (9) and (10). Furthermore only one stable s+g solution is present. We explain the details in the following.

First we consider a special case: $V_s = V_g = -V_{sg}$. Then, by adding Eqs. (9) and (10) one can immediately obtain the solution with $x = 1/2$ independent of temperature. This means that irrelevant of temperature s- and g-wave coexists always with equal amplitudes. This result is obvious because in this case the pairing interaction (5) can be simply factorized again into the form $f(\theta, \phi) * f(\theta', \phi')$ with fixed $x = 1/2$. Then only the gap amplitude $\Delta(T)$ is left. It decreases gradually with T and vanishes at the transition temperature T_c , as shown by the dashed line in the upper panel of Fig. 3 where $\tilde{V}_s = 0.2$ is used.

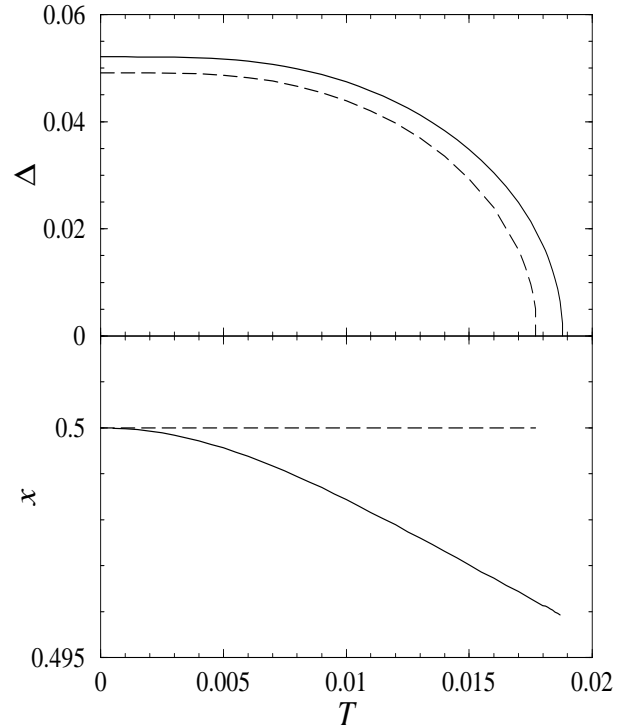


FIG. 3. The order parameter Δ and tuning parameter x as functions of temperature T . Δ and T are in units of $\hbar\omega_D$. The solid lines are for $\tilde{V}_s = 0.2$, $\tilde{V}_g = 0.1$, $\tilde{V}_{sg} = -0.22$, and the dashed lines are for $\tilde{V}_s = \tilde{V}_g = -\tilde{V}_{sg} = 0.2$ corresponding to the special case of T -independent $x = 1/2$ s+g wave.

Generally, the three interaction parameters have different absolute values. Various situations can be described by tuning these model parameters. We use the following strategy to obtain reasonable values: First, we fix the value of \tilde{V}_s , e.g. 0.2 throughout the work which sets the overall scale for T_c . Then we assume a value for \tilde{V}_g smaller than \tilde{V}_s and tune \tilde{V}_{sg} to realize the s+g state with the constraint: $x = 1/2$ at $T = 0$. Experimentally, the detection of nodes by the field angular-dependent thermal conductivity is applicable only at very low temperatures, i.e., $T \ll T_c$. Thus the measurement actually pro-

vides this constraint on the gap function. In this way, the value \tilde{V}_{sg} may be determined for each given \tilde{V}_g . We have obtained a nearly linear relation between \tilde{V}_{sg} and \tilde{V}_g : $\tilde{V}_{sg} \simeq -0.24 + 0.2\tilde{V}_g$. With interaction parameters fixed we can now study the intriguing issue how the $x = 1/2$ fine tuning s+g state at $T = 0$ evolves with temperature. One would expect that not only the gap amplitude Δ , but also the tuning parameter x will change with temperature. If it would decrease, the node points would cease to exist and a gap would open with increasing temperature. In principle this is indeed observed. As an example, we take $\tilde{V}_g = 0.1 < \tilde{V}_s$. Then $\tilde{V}_{sg} \simeq -0.22$ is obtained to realize the $x = 1/2$ s+g solution at $T = 0$. Under these interaction parameters, $\Delta(T)$ and $x(T)$ are calculated self-consistently from Eqs. (9) and (10). The results are shown by the solid lines in Fig. 3. It is interesting to see that x varies with T monotonically and very slowly. In the current example with $V_g < V_s$, x becomes less than $1/2$ at finite T . However, the deviation from $1/2$ is less than 1% even at $T = T_c$. This means that very strong anisotropic gap with $\Delta_{min}/\Delta_{max} \leq 10^{-2}$ is present in the whole superconducting region describing essentially still a gap with point nodes. Thus we conclude that s+g pairing with nodal excitations is a robust solution for all temperatures and should not be considered as accidental. We also mention that x becomes larger than $1/2$ at finite T for $V_g > V_s$ (not shown), but again only a small deviation is obtained.

IV. DISCUSSION AND CONCLUSION

In the above section, we have obtained the stable s+g-wave based on the phenomenological pairing interaction (5). Also we have realized the $x = 1/2$ hybrid state which has point nodes by appropriate choice of the interaction parameters, and most importantly have proven its robustness with temperature variation. A microscopic justification for our phenomenological scenario is yet to be investigated. On the other hand, we should return back to understand the form of the pairing potential Eq. (5) in more detail. This is discussed in the following.

For a system with full translation symmetry, the pairing potential $V_{\mathbf{k}\mathbf{k}'}$ can only be a function of $\mathbf{k} - \mathbf{k}'$. Further it may be considered to be a function of the angle between the two wavevectors in view of $|\mathbf{k}|, |\mathbf{k}'| \simeq k_F$ (the Fermi wave vector). Then $V_{\mathbf{k}\mathbf{k}'} = V(\hat{\mathbf{k}} \cdot \hat{\mathbf{k}'})$, with $\hat{\mathbf{k}} \cdot \hat{\mathbf{k}'}$ denoting the cosine of the angle between \mathbf{k} and \mathbf{k}' , can be expanded in terms of Legendre polynomials. And by use of the spherical harmonic addition theorem, it can be finally written into

$$V(\hat{\mathbf{k}} \cdot \hat{\mathbf{k}'}) = \sum_{l=0}^{\infty} V_l \sum_{m=-l}^l Y_{lm}(\theta, \phi) Y_{lm}^*(\theta', \phi') \quad (13)$$

through spherical harmonics $Y_{lm}(\theta, \phi)$. Obviously the V_s term corresponds to $l = 0$ and the V_g term results from

the sum of $(l, m) = (4, 4)$ and $(4, -4)$. However the cross term $\sim V_{sg}$ in Eq. (5) cannot be obtained from Eq. (13). This leads us to go beyond the above assumption, i.e., to consider $V_{\mathbf{k}\mathbf{k}'}$ as a general function which depends on \mathbf{k} and \mathbf{k}' individually. This will be the case when the effect of having only discrete lattice translation and rotation symmetry is included. Then the pair potential has to be expanded in terms of the basis functions $\psi_{\Gamma}^{i(l)}(\theta, \phi)$ of the crystal symmetry group (D_{4h}) belonging to a specific irreducible representation Γ of degree l and degeneracy index i . The generalized expansion then reads, suppressing the multiplicity index of Γ :

$$V_{\mathbf{k}\mathbf{k}'} = \sum_{\Gamma l'} V_{\Gamma}^{(l')} (k, k') \sum_i \psi_{\Gamma}^{i(l)}(\theta, \phi) \psi_{\Gamma}^{i(l')}(\theta', \phi')^*. \quad (14)$$

For basis functions of different degree l, l' but belonging to the same representation Γ the contribution will generally be nonzero. Then for $\Gamma = A_{1g}$ and $l = 0, l' = 4$ or vice versa one can naturally obtain the nondiagonal contributions $V_{A_{1g}}^{(04)} = V_{sg}$ in D_{4h} symmetry.

In conclusion, the s+g hybrid gap function has been studied within BCS theory. By an appropriate ansatz for the pairing interaction and selection of the interaction parameters we have shown that the stable coexistence of s- and g-wave, as well as the nodal state with equal amplitudes of them is possible. In particular, we have confirmed that the hybrid state with highly anisotropic gap may be robust in the whole superconducting region. This provides the semi-phenomenological theory to understand the s+g ($x = 1/2$) gap function proposed by Maki *et al.*¹⁴ Thus the explanation of the experimentally observed point nodes in borocarbides Y(Lu)Ni₂B₂C can be achieved in a self-consistent way. Finally we mention that similar s+g mixed gap functions are also proposed very recently for skutterudite PrOs₄Sb₁₂,²⁰ and their justification should be possible based on a similar analysis as presented here.

ACKNOWLEDGMENT

We thank J. Goryo, K. Maki, and Q. Gu for useful discussions. Q. Yuan also acknowledges the support by the National Natural Science Foundation of China (Grant No. 19904007).

¹ P.C. Canfield, P.L. Gammel, and D.J. Bishop, Phys. Today **51** (10), 40 (1998).

² *Rare Earth Transition Metal Borocarbides: Superconductivity, Magnetic and Normal State Properties*, edited by K.H. Müller and V. Narozhnyi (Kluwer Academic, Dordrecht, 2001).

- ³ S. A. Carter, B. Batlogg, R. J. Cava, J. J. Krajewski, W. F. Peck, and H. Takagi, Phys. Rev. B **50**, 4216 (1994); L. F. Mattheiss, *ibid.* **49**, 13279-13282 (1994); H. Michor, T. Holubar, C. Dusek, and G. Hilscher, *ibid.* **52**, 16165 (1995).
- ⁴ M. Nohara, M. Isshiki, H. Takagi, and R. J. Cava, J. Phys. Soc. Jpn. **66**, 1888 (1997).
- ⁵ M. Nohara, M. Isshiki, F. Sakai, and H. Takagi, J. Phys. Soc. Jpn. **68**, 1078 (1999).
- ⁶ K. Izawa, A. Shibata, Yuji Matsuda, Y. Kato, H. Takeya, K. Hirata, C. J. van der Beek, and M. Konczykowski, Phys. Rev. Lett. **86**, 1327 (2001).
- ⁷ T. Park, M. B. Salamon, E. M. Choi, H. J. Kim, S. I. Lee, cond-mat/0210145.
- ⁸ K. Izawa, K. Kamata, Y. Nakajima, Y. Matsuda, T. Watanabe, M. Nohara, H. Takagi, P. Thalmeier, and K. Maki, Phys. Rev. Lett. **89**, 137006 (2002).
- ⁹ E. Boaknin, R. W. Hill, C. Proust, C. Lupien, and L. Taillefer, and P. C. Canfield, Phys. Rev. Lett. **87**, 237001 (2001).
- ¹⁰ I. S. Yang, M. V. Klein, S. L. Cooper, P. C. Canfield, B. K. Cho, and S. I. Lee, Phys. Rev. B **62**, 1291 (2000).
- ¹¹ G.-Q. Zheng, Y. Wada, K. Hashimoto, Y. Kitaoka, K. Asayama, H. Takeya, and K. Kadowaki, J. Phys. Chem. Solids **59**, 2169 (1998).
- ¹² T. Yokoya, T. Kiss, T. Watanabe, S. Shin, M. Nohara, H. Takagi, and T. Oguchi, Phys. Rev. Lett. **85**, 4952 (2000).
- ¹³ P. Martínez-Samper, H. Suderow, S. Vieira, J. P. Brison, N. Luchier, P. Lejay, P. C. Canfield, cond-mat/0209469.
- ¹⁴ K. Maki, P. Thalmeier, and H. Won, Phys. Rev. B **65**, R140502 (2002).
- ¹⁵ P. Thalmeier and K. Maki, cond-mat/0210364.
- ¹⁶ S. B. Dugdale, M. A. Alam, I. Wilkinson, R. J. Hughes, I. R. Fisher, P. C. Canfield, T. Jarlborg, and G. Santi, Phys. Rev. Lett. **83**, 4824 (1999).
- ¹⁷ H. C. Lee and H. Y. Choi, Phys. Rev. B **65**, 174530 (2002).
- ¹⁸ A. Ghosh and S. K. Adhikari, Physica C **355**, 77 (2001); **370**, 146 (2002).
- ¹⁹ Only in a narrow region about $1.07 < \tilde{V}_g < 1.08$, the dotted line, which is indiscernible from the solid one, has the lowest energy, indicating a stable s+g solution with $x \approx 1$.
- ²⁰ K. Maki, P. Thalmeier, Q. Yuan, K. Izawa, and Y. Matsuda, cond-mat/0212090.